Article

Discovery Medicine 2026; 38(205): 540–552
https://doi.org/10.24976/Discov.Med.202638205.45

From Methylation to Mitochondrial Collapse: Unraveling the CTCF-EP300/MTHFD2 Pathway in Sepsis-Induced Acute Kidney Injury

Weike Hu[1,*]

[1]Emergency Department, The First Affiliated Hospital of Ningbo University, 315020 Ningbo, Zhejiang, China
*Correspondence: fyyhuweike@nbu.edu.cn (Weike Hu)
Submitted: 18 November 2025 Revised: 7 January 2026 Accepted: 20 January 2026 Published: 20 February 2026

Background: Sepsis-induced acute kidney injury (AKI) is a severe clinical complication characterized by tubular epithelial cell damage and mitochondrial dysfunction. This study aims to elucidate the mechanism by which methylation of CCCTC-binding factor (CTCF) regulates the E1A binding protein p300 (EP300)/methylenetetrahydrofolate dehydrogenase (NADP+ dependent) 2 (MTHFD2) axis and, as a result, impacts mitochondrial function during septic tubular injury.

Methods: Human renal proximal tubular epithelial HK-2 cells were treated with lipopolysaccharide (LPS) to mimic septic conditions. The regulatory relationship between CTCF methylation and the EP300/MTHFD2 axis was analyzed using luciferase reporter assays, chromatin immunoprecipitation (ChIP), co-immunoprecipitation (Co-IP), and methylation-specific PCR (MSP). Cell viability, apoptosis, reactive oxygen species (ROS) levels, and mitochondrial membrane potential were assessed through 3-(4,5-dimethylthiazol-2-yl)-2,5-diphenyl tetrazolium bromide (MTT) assays, terminal deoxynucleotidyl transferase dUTP nick end labeling (TUNEL) staining, flow cytometry, and JC-1 staining, respectively.

Results: CTCF interacted with EP300 and impacted the expression of MTHFD2 ($p < 0.01$). Knockdown of CTCF resulted in MTHFD2 downregulation and decreased H3K27ac enrichment at the MTHFD2 promoter ($p < 0.001$). EP300 regulated MTHFD2 transcription by promoting histone H3 lysine 27 acetylation (H3K27ac) at its promoter ($p < 0.05$). Functional experiments demonstrated that CTCF silencing exacerbated LPS-induced weakened viability, increased apoptosis, elevated ROS production, and decreased mitochondrial membrane potential ($p < 0.001$). Notably, EP300 overexpression reversed these pathological changes ($p < 0.001$). Furthermore, the methylation status of the CTCF promoter was influenced by MTHFD2 expression ($p < 0.05$).

Conclusion: This *in vitro* study reveals a novel regulatory axis in which methylation of CTCF modulates the EP300/MTHFD2 pathway, which may contribute to mitochondrial dysfunction in tubular epithelial cells (HK-2) under septic conditions.

Keywords: sepsis; acute kidney injury; CCCTC-binding factor; methylation; mitochondrial dysfunction

Introduction

Sepsis is a life-threatening illness attributed to infection-induced systemic inflammatory response syndrome (SIRS), typically leading to numerous organ failures and posing a major threat to patient's survival [1]. Despite advances in medical care, sepsis remains associated with high morbidity and mortality rates, and its complications contribute to approximately 11 million deaths globally each year [2]. Acute kidney injury (AKI), one of the most common and severe complications of sepsis, is defined as a rapid decline in renal function [3], which is mechanistically associated with impaired energy metabolism [4,5]. As the central organelle of cellular energy production, mitochondrial dysfunction plays a critical role in the pathogenesis of septic AKI [6,7]. For instance, Wang *et al.* [8] reported that the PTEN-induced kinase 1 (PINK1)/parkin RBR E3 ubiquitin protein ligase (PARK2)/optineurin-mediated mitophagy pathway is activated in sepsis-induced kidney injury, thereby alleviating tubular epithelial cell damage. Moreover, Ye *et al.* [9] demonstrated that circular RNA itchy E3 ubiquitin protein ligase ameliorates mitochondrial dysfunction in septic AKI by modulating the microRNA-214-3p/adenosine triphosphate (ATP) binding cassette subfamily A member 1 (ABCA1) axis. These findings highlight the therapeutic potential of restoring mitochondrial function in attenuating sepsis-associated kidney injury.

In our previous study, we conducted a comprehensive transcriptomic analysis of sepsis-related renal tissues using dataset GSE60088, and identified methylenetetrahydrofolate dehydrogenase (NADP + dependent) 2 (MTHFD2) as a gene of particular interest. MTHFD2, a folate cycle enzyme, is localized to the mitochondria, and primarily expressed in embryonic tissues and rapidly proliferating cells [10]. In addition to its role in one-carbon metabolism, MTHFD2 supports mitochondrial respiratory chain integrity, thereby preventing mitochondrial dysfunction and mitigating oxidative stress and apoptosis-related

Table 1. Sequences of small interfering RNAs (siRNAs).

Genes	Sense (5′-3′)	Antisense: (5′-3′)
siCTCF#1	GAGUAAACGUGGAAGAAAAUU	UUUUCUUCCACGUUUACUCUU
siCTCF#2	GAGAAACGAAGAAGAGUAA	UUACUCUUCUUCGUUUCUC
siCTCF#3	GGAGAAACGAAGAAGAGUA	UACUCUUCUUCGUUUCUCC
siMTHFD2#1	CCAAAGAGCAGUUGAAGAAUU	UUCUUCAACUGCUCUUUGGUU
siMTHFD2#2	UGGCAAUGCUAAUGAAGAAUU	UUCUUCAUUAGCAUUGCCAUU
siMTHFD2#3	GAGAAGUGCUGAAGUCUAAUU	UUAGACUUCAGCACUUCUCUU
siNC	UUCUCCGAACGUGUCACGUTT	ACGUGACACGUUCGGAGAATT

CTCF, CCCTC-binding factor; MTHFD2, methylenetetrahydrofolate dehydrogenase (NADP+ dependent) 2; NC, negative control.

injury [11,12]. MTHFD2 is an enzyme involved in folate metabolism, and inhibition of folate metabolism severely damages kidney structurally and functionally [13]. Our investigation also revealed significant enrichment of E1A binding protein p300 (EP300) (a histone acetyltransferase) at the promoter region of MTHFD2. EP300 is a well-established chromatin remodeling factor known to play a central regulatory role in the pathogenesis of AKI [14]. A key mechanism by which EP300 activates transcription is through catalyzing the acetylation of histone H3 at lysine 27 (H3K27ac), a hallmark of active enhancers and promoters [15]. Another key regulator gene is CCCTC-binding factor (CTCF), a multifunctional DNA-binding protein involved in chromatin architecture, promoter-enhancer looping, and transcription factor recruitment [16]. Emerging evidence suggests that CTCF can directly recruit EP300 to target gene promoters to regulate transcription [17]. Notably, the binding affinity of CTCF to its target genes is markedly enhanced under septic conditions [18], suggesting its pivotal role in the regulation of inflammation-related gene expression.

As an essential epigenetic mechanism, DNA methylation plays a critical role in the pathophysiology of inflammatory diseases, including sepsis [19]. Folate, a major methyl group donor required for DNA methylation, is closely linked to the cellular methylation status [20]. Through bioinformatic analysis, we identified a prominent CpG island in the promoter region of the CTCF gene, indicating that it may be impacted by DNA methylation. In this study, we aim to investigate the role and underlying mechanisms of the CTCF methylation mediating EP300/MTHFD2 axis in mitochondrial dysfunction of tubular epithelial cells during sepsis-induced AKI, with a particular focus on the epigenetic regulation of CTCF promoter methylation.

Materials and Methods

Cell Culture

Human renal proximal tubular epithelial cells (HK-2; AW-CH0140, AnWei-sci, Shanghai, China) were cultivated in Dulbecco's Modified Eagle Medium (DMEM; 11965126, Thermo Fisher Scientific, Waltham, MA, USA) with 1% penicillin-streptomycin (C0222, Beyotime, Shanghai, China) and 10% heat-inactivated fetal bovine serum (FBS; C0235, Beyotime, Shanghai, China). The cells were kept at 37 °C in a humidified incubator (Forma Steri-Cult, Thermo Fisher Scientific, Waltham, MA, USA) with 5% CO_2. The HK-2 cells were verified by short tandem repeat (STR) profiling. A model of sepsis-induced AKI was created in HK-2 cells by 6-hour treatment with 10 µg/mL lipopolysaccharide (LPS; HY-D1056, MedChemExpress, Monmouth Junction, NJ, USA) [21]. Cell lines were negative for mycoplasma.

Cell Transfection

GenePharma (China) synthesized small interfering RNAs (siRNAs) that targeted CTCF (siCTCF#1, siCTCF#2, siCTCF#3) and MTHFD2 (siMTHFD2#1, siMTHFD2#2, siMTHFD2#3), as well as negative control siRNA (siNC). The siRNA sequences are listed in Table 1. The full length of EP300 [NM_001429.4] and CTCF [NM_006565.4] was cloned into the pcDNA3.1 vector (VT1001, Youbio, Changsha, China) to obtain overexpression plasmids, the corresponding empty vector was used as the negative control (NC). As directed by the manufacturer, Lipofectamine 2000 (11668019, Invitrogen, Carlsbad, CA, USA) was employed for the transfections. After transfection, the cells were cultured for 48 hours. Reverse transcription quantitative polymerase chain reaction (RT-qPCR) was applied to verify the effectiveness of the transfection.

Cell Grouping

HK-2 cells were classified into the following categories: Control, LPS, LPS+siNC+NC, LPS+siCTCF+NC, LPS+siCTCF+EP300, LPS+5-Aza-2′-deoxycytidine (5-Aza), LPS+siMTHFD2+NC, and LPS+siMTHFD2+CTCF. 10 µg/mL LPS treatment was administered for 6 hours in the LPS and LPS+5-Aza groups. Additionally, cells in the LPS+5-Aza group received a 72-hour pretreatment with 15.5 nM 5-Aza (HY-A0004, MedChemExpress, Monmouth Junction, NJ, USA) [22], a potent DNA methyltransferase inhibitor that promotes DNA demethylation [23]. After

Table 2. Primers used for real-time PCR in this study.

Genes	Forward primer (5′-3′)	Reverse primer (5′-3′)	Note
MTHFD2	CCCAGCAGATCAAGCAGGAA	GCTGCCCTGGTTTTGTTGAG	qRT-PCR
CTCF	CAGCCACGGAGAGGTACTCG	GCTGACTTCTACACTGGCGT	
EP300	ACCAGGAATGACTTCTAGTTTGA	TACGAGGCCCATAGCCCATA	
β-actin	CATGTACGTTGCTATCCAGGC	CTCCTTAATGTCACGCACGAT	
CTCF-M	TTTCGACGTTGCGTGTAGT	GACGATACGAAATCGACGA	MSP
CTCF-U	TTTTGATGTTGTGTGTAGT	AACATACAAAATCAACAA	

EP300, E1A binding protein p300.

Table 3. Antibodies used in western blot analysis.

Antibody name	Molecular weight	Source	Catalog number	Supplier	Type	Dilution
EP300	264 kDa	Rabbit	ab259330	Abcam, Cambridge, UK	Primary antibody	1:1000
CTCF	83 kDa	Rabbit	ab300639	Abcam, Cambridge, UK	Primary antibody	1:1000
MTHFD2	35 kDa	Rabbit	ab307428	Abcam, Cambridge, UK	Primary antibody	1:1000
β-actin	42 kDa	Mouse	ab8226	Abcam, Cambridge, UK	Primary antibody	1:1000
Goat Anti-Rabbit IgG H&L (HRP)			ab6721	Abcam, Cambridge, UK	Secondary antibody	1:4000
Goat Anti-Mouse IgG H&L (HRP)			ab205719	Abcam, Cambridge, UK	Secondary antibody	1:4000

CTCF, CCCTC-binding factor; EP300, E1A binding protein p300; MTHFD2, methylenetetrahydrofolate dehydrogenase (NADP+ dependent) 2.

transfection with the proper siRNAs and plasmids, the cells were cultured for 48 hours and then stimulated with 10 µg/mL of LPS for 6 hours.

qRT-PCR

Cells were treated with TRIzol reagent (R0016, Beyotime, Shanghai, China) to extract total RNA. The amount of RNA was then detected with a spectrophotometer (Biochrom Ltd., Cambridge, UK). In accordance with the manufacturer's instructions, complementary DNA (cDNA) was synthesized employing the HiScript® III RT SuperMix (R323-01, Vazyme, Nanjing, China). Next, RT-qPCR was carried out on a 7500 Real-Time PCR System (Applied Biosystems, Waltham, MA, USA), using a SYBR® qPCR master mix (4344463, Thermo Fisher Scientific, Waltham, MA, USA) and specific primers (Table 2, Tsingke, China). *β*-actin served as an internal control. The $2^{-\Delta\Delta Ct}$ technique was implemented to calculate relative mRNA expression levels.

Western Blot Analysis

Radioimmunoprecipitation assay (RIPA) buffer (P0013, Beyotime, Shanghai, China) was employed to lyse HK-2 cells, and cell lysates were centrifuged to collect the supernatants. The Bradford assay (C503031, Sangon Biotech, Beijing, China) was then applied to measure the quantities of proteins. Equal quantities of protein (35 µg per lane) were separated using 10% sodium dodecyl sulfate-polyacrylamide gel electrophoresis (SDS-PAGE; P0690, Beyotime, Shanghai, China), and then transferred onto polyvinylidene fluoride (PVDF) membranes (FFP24, Beyotime, Shanghai, China). Afterwards, the membranes were blocked utilizing 5% non-fat milk, incubated with primary antibodies (Table 3) overnight at 4 °C, washed and cultured for 1 hour at room temperature with the relevant secondary antibodies (Table 3). Using a gel documentation system (Bio-Rad, Hercules, CA, USA) and an enhanced chemiluminescence detection kit (KGC4902, KeyGene, Nanjing, China), protein bands were observed. ImageJ software (version 1.47, NIH, Bethesda, MD, USA) was employed to quantify grayscale intensity of the bands.

Luciferase Reporter Assay

A firefly luciferase reporter plasmid was constructed by cloning a ~1.5 kb fragment of the human MTHFD2 gene promoter (spanning approximately –1500 to +100 bp relative to the transcription start site) into the pGL4-basic luciferase vector (TM259, Promega, Madison, WI, USA). For the assay, HK-2 cells were seeded in 24-well plates and transfected at 70–80% confluence. Each well was co-transfected with 0.4 µg of the pGL4-MTHFD2-promoter reporter plasmid using Lipofectamine 2000 transfection reagent, according to the manufacturer's protocol. Transfected cells were divided into two treatment groups: Vehicle and EP300 inhibitor (C646). The cells in the C646 group were treated with 10 µM C646 (HY-13823, MCE, Monmouth Junction, NJ, USA) [24], while the cells in the Vehicle group were maintained under standard culture conditions. Following the manufacturer's instructions, luciferase activity was assessed 48 hours after transfection utilizing the Dual-Luciferase Reporter Assay System (E1910, Promega, Madison, WI, USA).

Chromatin Immunoprecipitation (ChIP)

For investigating the relationship between MTHFD2 and acetylated histone H3 at lysine 27 (H3K27ac) or EP300, ChIP was carried out using a commercial kit (9003, Cell Signaling Technology, Boston, MA, USA). While the HK-2 cells in the C646 group were treated with 10 μM C646 (HY-13823, MCE, Monmouth Junction, NJ, USA) [24], the cells in the Vehicle group were maintained under standard culture conditions. HK-2 cells were then cross-linked for 15 minutes using 1% formaldehyde (C06701102, Nanjing Reagent, Nanjing, China), after which micrococcal nuclease was used to lyse the cells and break up the chromatin. Next, Anti-H3K27ac (ab4729, Abcam, Cambridge, UK), anti-EP300 (ab275378, Abcam, Cambridge, UK), or control IgG (ab216352, Abcam, Cambridge, UK) was applied to immunoprecipitate the chromatin at 4 °C overnight, and the chromatin was incubated with ChIP-grade Protein G magnetic beads. Following successive washing, spin columns were utilized to purify the DNA and reverse the cross-links. Quantitative PCR (qPCR) was conducted to examine the enrichment of H3K27ac or EP300 at the MTHFD2 promoter using the following MTHFD2 primers: Forward: 5′-CTCAACAAAACCAGGGCAGC-3′; Reverse: 5′-TGCTCTGGAAGAGGCAACTG-3′.

Co-Immunoprecipitation (Co-IP)

Cells were collected and lysed with RIPA buffer. A 5-fold dilution of protein lysate in immunoprecipitation (IP) buffer (P0013, Beyotime, Shanghai, China) containing phenylmethylsulfonyl fluoride (PMSF, ST506, Beyotime, Shanghai, China) was used for each IP process, and the total protein concentration was measured. Protein G agarose beads (PR40025, Proteintech, Wuhan, China) were added to pre-wash the lysates for 2 hours at 4 °C. Primary antibodies were added to the centrifuged supernatants for overnight incubation (4 °C): anti-CTCF (ab300639, Abcam, Cambridge, UK), anti-EP300 (ab275378, Abcam, Cambridge, UK), or control IgG (ab216352, Abcam, Cambridge, UK). To collect immune complexes, fresh Protein G agarose beads were added and gently rotated for two hours at 4 °C. The beads were centrifuged after being washed three times with IP buffer and once with IP buffer containing 0.1% Triton X-100. Next, the beads were boiled in 25 μL of 2× sodium dodecyl sulfate (SDS) loading buffer (LC2676, ThermoFisher, Waltham, MA, USA) for 10 minutes at 100°C to elute bound proteins. Following centrifugation, the supernatants were collected and underwent the previously mentioned Western blot procedure.

Cell Viability Assay

A commercial 3-(4,5-dimethylthiazol-2-yl)-2,5-diphenyl tetrazolium bromide (MTT) test kit (C0009S, Beyotime, Shanghai, China) was applied to evaluate cell viability in accordance with the manufacturer's instructions. After being seeded into 96-well plates (FUV961, Beyotime, Shanghai, China), HK-2 cells (2×10^4 per well) were treated, and cultivated with 10 μL of MTT solution for 4 hours in darkness. Absorbance at 570 nm was measured using an Elx800 microplate reader (Bio-Tek, Winooski, VT, USA).

Cell Apoptosis Assay

Using the *In Situ* Cell Death Detection Kit (C1086, Beyotime, Shanghai, China), terminal deoxynucleotidyl transferase dUTP nick end labeling (TUNEL) staining was carried out in accordance with the manufacturer's instructions to evaluate cell apoptosis. HK-2 cells were seeded on glass coverslips on 6-well plates (BS-CP-6C, Biosharp, Beijing, China) and then exposed to specified treatments. After 15-minute fixation with 4% paraformaldehyde (P0099, Beyotime, Shanghai, China), cells were permeabilized using 0.3% Triton X-100 (10 minutes), washed with phosphate-buffered saline (PBS; C0221A, Beyotime, Shanghai, China) and then incubated for 1 hour (37 °C) with 50 μL of TUNEL reaction mixture. 2-(4-amidinophenyl)-6-indolecarbamidine dihydrochloride (DAPI; C1002, Beyotime, Shanghai, China) was then applied to counterstain the nuclei for 10 minutes at room temperature. A fluorescent microscope (Nikon, Tokyo, Japan; 200×) was employed to acquire the images. Nuclei that were positive for DAPI fluoresced blue, whereas cells that were positive for TUNEL fluoresced green. The number of apoptotic cells was determined by counting TUNEL-positive cells using ImageJ software (version 1.47, NIH, Bethesda, MD, USA).

Reactive Oxygen Species (ROS) Measurement

HK-2 cells (1×10^5 cells/well) were planted in 6-well plates (FCP060, Beyotime, Shanghai, China) for 24 hours, after which the cells were digested in Trypsin (40101ES25, Yeasen, Shanghai, China), washed with PBS twice, and collected. Next, the cells were treated for 30 minutes with 10 μM 2′,7′-dichlorofluorescein diacetate (DCFH-DA; S0033l, Beyotime, Shanghai, China), rinsed three times in serum-free media to remove extra DCFH-DA, and resuspended in 1 mL PBS. A FACS Calibur flow cytometer (Becton-Dickinson Biosciences, San Jose, CA, USA) was used to measure the intracellular ROS levels.

Mitochondrial Membrane Potential (MMP)

Following treatment, the cells were washed three times with prewarmed PBS, and the culture media were removed. Cells were then treated with 200 nM JC-1 dye (C2006, Beyotime, Shanghai, China) for 30 minutes at 37 °C based on the manufacturer's instructions. A fluorescence microscope (200×) was utilized to observe the red and green fluorescence. JC-1 remained in its monomeric state and emitted green fluorescence in mitochondria with low membrane potential, while producing red-fluorescent J-aggregates in mitochondria with high membrane potential. The fluorescence intensity ratio of red to green

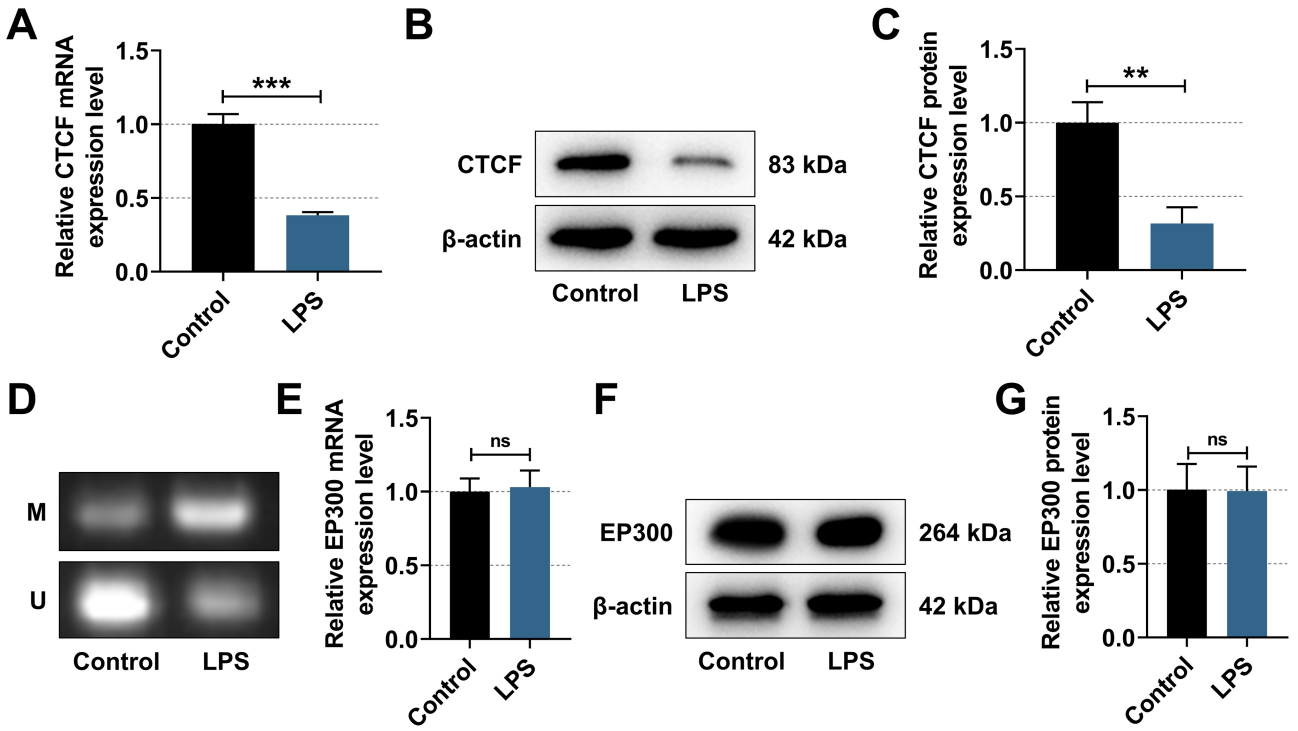

Fig. 1. Lipopolysaccharide (LPS) stimulation significantly downregulated the expression of CCCTC-binding factor (CTCF) at both mRNA and protein levels. (A) Quantitative reverse transcription PCR (qRT-PCR) analysis of the expression of *CTCF* after LPS stimulation in HK-2 cells. *β-actin* was used as the internal control. (B,C) Western blot analysis of CTCF protein levels in LPS-treated HK-2 cells. β-actin was used as the loading control. (D) Methylation-specific PCR analysis of CTCF methylation levels in HK-2 cells from the control and LPS groups. (E) qRT-PCR analysis of the expression of E1A binding protein p300 (EP300) after LPS stimulation in HK-2 cells. β-actin was used as the internal control. (F,G) Western blot analysis of EP300 protein levels in LPS-treated HK-2 cells. β-actin was used as the loading control. All experiments were independently repeated three times. $^{**}p < 0.01$, $^{***}p < 0.001$. ns, no significance.

was quantified using ImageJ software (version 1.47, NIH, Bethesda, MD, USA) to evaluate changes in mitochondrial membrane potential.

Methylation-Specific PCR (MSP)

Genomic DNA of HK-2 cells was extracted with the QIAamp DNA Mini Kit (51304, Haoranbio, Shanghai, China), and converted to bisulfite using Epitect Fast DNA Bisulfite Kit (59824, Bjingbio, Shanghai, China). QPCR, as described above, was applied to determine the methylation levels of the CTCF. The primers are listed in Table 2.

Statistical Analysis

The software GraphPad Prism version 8.0 (GraphPad, La Jolla, CA, USA) was employed to conduct statistical analyses. All experiments were independently repeated three times. Data were displayed as mean ± standard deviation (SD). Differences between two groups were examined by an unpaired Student's *t*-test. Tukey's post hoc test was employed after one-way analysis of variance (ANOVA) for comparisons between multiple groups. *p*-values below 0.05 were regarded as statistically significant.

Results

CTCF Recruited EP300 to Bind the MTHFD2 Promoter

To investigate the role of CTCF in septic AKI, we first examined its expression in renal tubular epithelial cells under LPS challenge. We found that LPS stimulation significantly downregulated both mRNA and protein levels of CTCF (Fig. 1A–C, $p < 0.01$). Concurrently, MSP revealed a substantial increase in DNA methylation at the CTCF promoter (Fig. 1D), suggesting epigenetic repression of CTCF in LPS treatment. We then assessed the expression of EP300, a key transcriptional coactivator. Interestingly, LPS treatment did not significantly alter EP300 levels (Fig. 1E–G).

Moreover, the effect of *CTCF* knockdown on *EP300* and *MTHFD2* expression was explored. First, compared to siNC, siCTCF#1, siCTCF#2, and siCTCF#3 all greatly lowered CTCF levels, with siCTCF#2 exerting the strongest impacts, and was therefore chosen for further research (Fig. 2A, $p < 0.001$). Then, qRT-PCR and Western blot results showed that knockdown of CTCF resulted in a

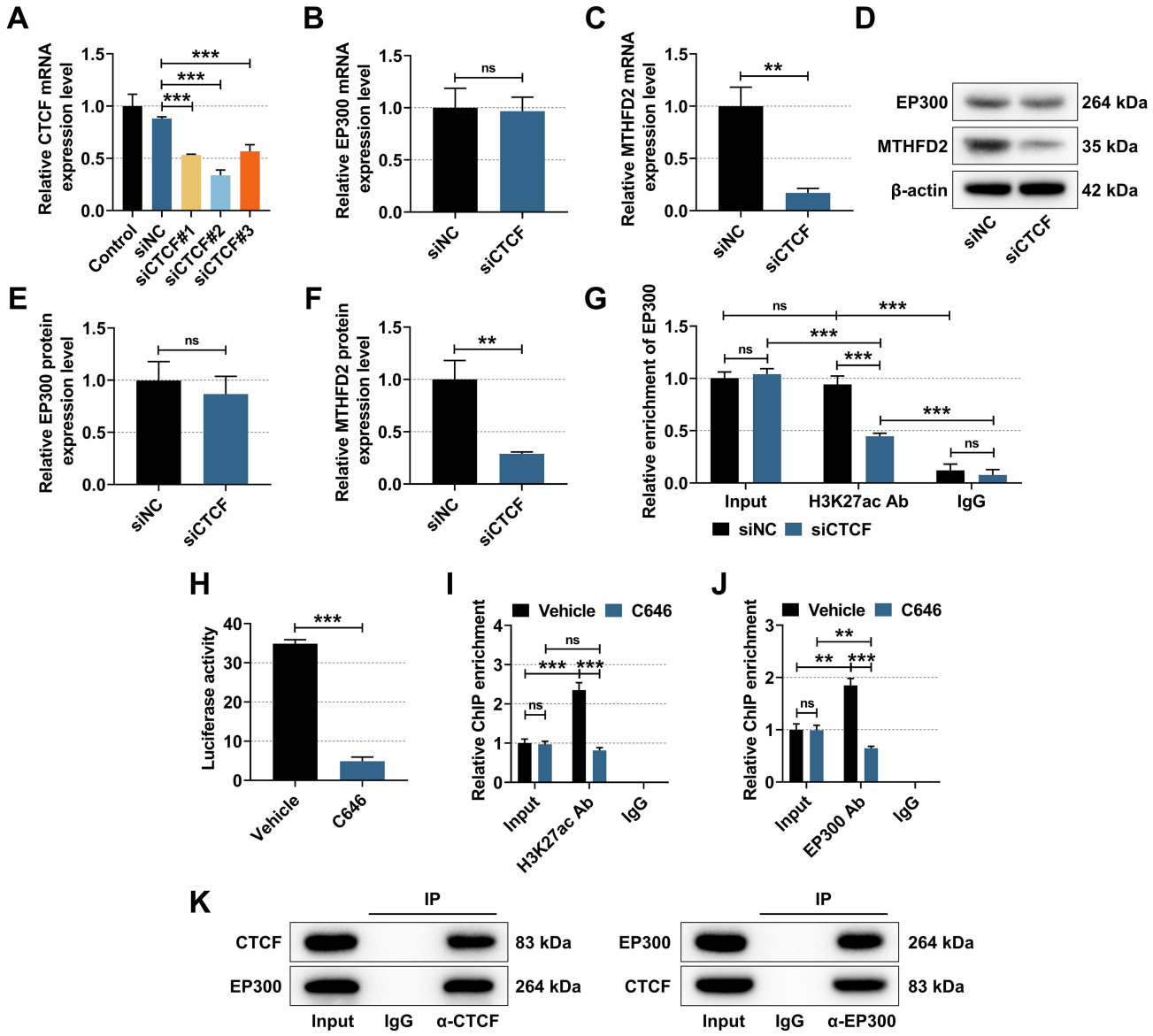

Fig. 2. Methylenetetrahydrofolate dehydrogenase (NADP+ dependent) 2 (MTHFD2) was regulated by E1A binding protein p300 (EP300)-mediated histone H3 acetylated at lysine 27 (H3K27ac) modification. (A) Quantitative reverse transcription PCR (qRT-PCR) analysis of small interfering RNA (siRNA)-mediated *CTCF* (siCTCF) knock-down efficiency in HK-2 cells. *β-actin* was used as the internal control. (B,C) qRT-PCR analysis of *EP300* and *MTHFD2* mRNA levels in HK-2 cells transfected with control siRNA (siNC) or siCTCF. *β-actin* served as the internal control. (D–F) Western blot analysis of EP300 and MTHFD2 protein levels in siNC- and siCTCF-transfected HK-2 cells. β-actin was used as the loading control. (G) ChIP assay to examine the interaction between H3K27ac and the MTHFD2 promoter in HK-2 cells transfected with siNC or siCTCF. (H) Luciferase activity of the MTHFD2 promoter in HK-2 cells treated with or without the EP300 inhibitor C646. (I,J) Chromatin immunoprecipitation (ChIP) assays to detect the interaction between (I) Histone H3 lysine 27 acetylation (H3K27ac) or (J) EP300 and the MTHFD2 promoter in HK-2 cells. (K) Co-immunoprecipitation (Co-IP) analysis of the interaction between CCCTC-binding factor (CTCF) and EP300. All experiments were independently repeated three times. $^{**}p < 0.01$, $^{***}p < 0.001$. ns, no significance.

significant downregulation of MTHFD2 at both the mRNA and protein levels, whereas the expression levels of EP300 (mRNA and protein) were not affected (Fig. 2B–F). To directly assess the functional outcome of EP300 recruitment, we measured the level of the active histone mark H3K27ac at the MTHFD2 promoter by chromatin immunoprecipitation (ChIP) using an H3K27ac-specific antibody. This approach is based on the established role of EP300 as a major histone acetyltransferase that catalyzes H3K27 acetylation [25]. The results showed that knockdown of CTCF significantly diminished the enrichment of H3K27ac at the MTHFD2 promoter (Fig. 2G, $p < 0.001$).

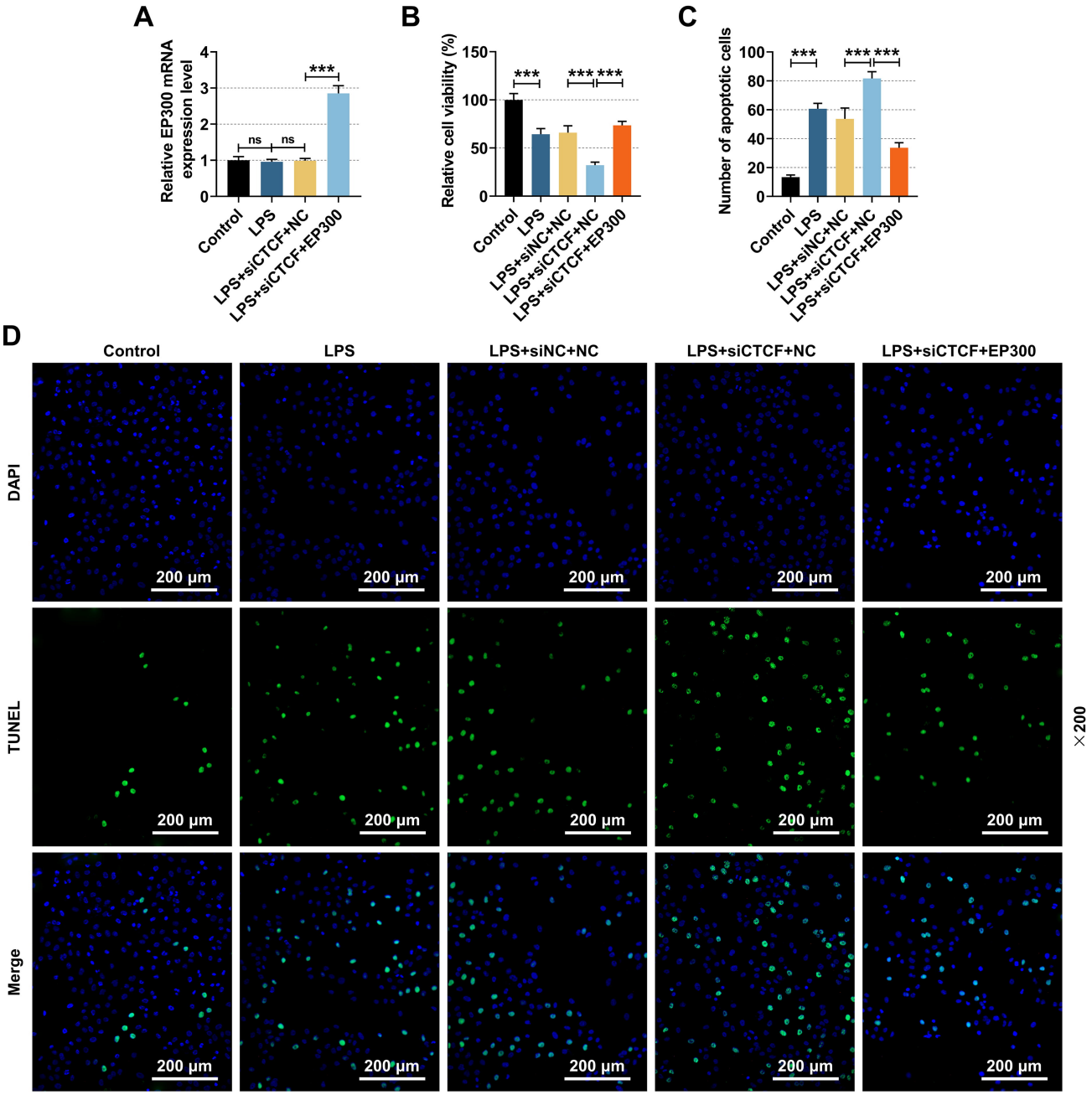

Fig. 3. CTCF and EP300 regulated lipopolysaccharide (LPS)-induced HK-2 cell viability and apoptosis. (A) qRT-PCR analysis of *EP300* overexpression efficiency in HK-2 cells. *β-actin* was used as the internal control. (B) 3-(4,5-dimethylthiazol-2-yl)-2,5-diphenyl tetrazolium bromide (MTT) assay to assess cell viability among the Control, LPS, LPS+siNC+negative control (NC), LPS+siCTCF+NC, and LPS+siCTCF+EP300 groups. (C,D) Terminal deoxynucleotidyl transferase dUTP nick end labeling (TUNEL) assay to evaluate cell apoptosis across the same groups. Green indicates TUNEL-positive cells; magnification: 200×; scale bar = 200 μm. All experiments were independently repeated three times. $^{***}p < 0.001$. ns, no significance.

We next sought direct evidence that EP300's catalytic activity regulates MTHFD2 transcription. HK-2 cells were transfected with pGL3-basic plasmids carrying the MTHFD2 promoter sequence and treated with or without C646 to examine the relationship between EP300 and MTHFD2. According to the results of the Luciferase reporter experiment, C646 dramatically reduced the MTHFD2 promoter's activity (Fig. 2H, $p < 0.001$). H3K27ac and EP300 were strongly enriched at the MTHFD2 promoter in HK-2 cells, as described in ChIP data (Fig. 2I,J, $p < 0.001$). Co-IP outcomes demonstrated that CTCF and EP300 had a strong interaction (Fig. 2K). Thus, CTCF acts as a critical upstream regulator that facilitates EP300-dependent transcriptional activation of MTHFD2.

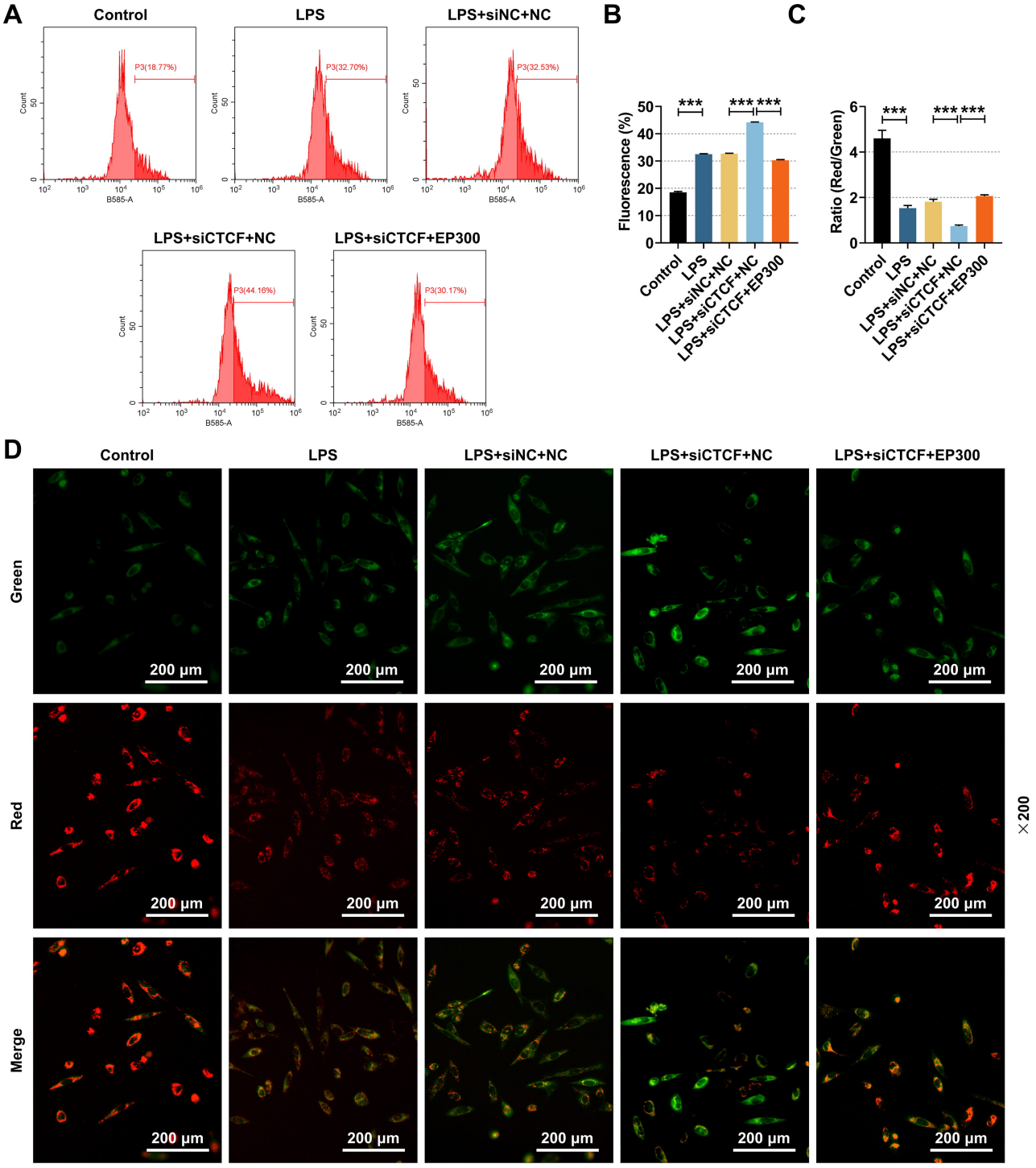

Fig. 4. CTCF and EP300 mediated LPS-induced reactive oxygen species (ROS) production and mitochondrial membrane potential in HK-2 cells. (A,B) Flow cytometry analysis of ROS levels in the Control, LPS, LPS+siNC+NC, LPS+siCTCF+NC, and LPS+siCTCF+EP300 groups. (C,D) JC-1 staining to assess mitochondrial membrane potential in the Control, LPS, LPS+siNC+NC, LPS+siCTCF+NC, and LPS+siCTCF+EP300 groups. Magnification: 200×; scale bar = 200 μm. All experiments were independently repeated three times. $^{***}p < 0.001$.

EP300 Overexpression Reversed the Effects of CTCF Silencing on LPS-Induced Injury

EP300 expression was considerably higher in the EP300 overexpression group than in the NC group (Fig. 3A, $p < 0.001$). In HK-2 cells, LPS treatment significantly reduced MMP and cell viability ($p < 0.001$), while enhancing ROS ($p < 0.001$) and apoptosis (green fluorescence) (Fig. 3B–D and Fig. 4A–D). Notably, the relative cell vi-

ability of LPS+siCTCF+NC showed a significant decrease compared to LPS+siNC+NC (Fig. 3B, $p < 0.001$), while compared to LPS+siCTCF+NC, the relative cell viability was significant higher in LPS+siCTCF+EP300 (Fig. 3B, $p < 0.001$).

Further, the number of apoptotic cells of LPS+siCTCF+NC showed a significant increase compared to LPS+siNC+NC (Fig. 3C,D, $p < 0.001$), while compared to LPS+siCTCF+NC, the number of apoptotic cells was significantly lower in LPS+siCTCF+EP300 (Fig. 3C,D, $p < 0.001$). Moreover, under LPS condition, siCTCF treatment increased ROS level and decreased membrane potential, which were reversed by EP300 overexpression (Fig. 4A–D, $p < 0.001$). This demonstrates that EP300 overexpression rescues mitochondrial and cellular injury induced by CTCF knockdown in LPS-treated HK-2 cells.

MTHFD2 Silencing Altered CTCF Promoter Methylation in LPS-Induced Cellular Injury

Compared to siNC, all three siRNAs targeting *MTHFD2* greatly lowered *MTHFD2* expression, and since siMTHFD2#1 had the most profound impact, it was thus employed for subsequent studies (Fig. 5A, $p < 0.001$). In HK-2 cells, LPS stimulation drastically reduced the expression of both CTCF and MTHFD2, an effect that was partially offset by 5-Aza, a DNA methyltransferase inhibitor (Fig. 5B–D, $p < 0.001$). In LPS-treated cells, MTHFD2 knockdown further reduced the expressions of both CTCF and MTHFD2, but these effects were counteracted by CTCF overexpression (Fig. 5B–D, $p < 0.05$). According to MSP data, LPS considerably raised CTCF methylation (Fig. 5E), 5-Aza therapy lessened the hypermethylation caused by LPS, and MTHFD2 knockdown also reversed the rise in CTCF DNA methylation (Fig. 5E). LPS substantially reduced cell viability (Fig. 5F, $p < 0.01$), enhanced apoptosis (Fig. 5G,H, $p < 0.001$) and ROS formation (Fig. 6A,B, $p < 0.001$) in HK-2 cells while functionally reducing MMP (Fig. 6C,D, $p < 0.001$). These effects were partially reversed by 5-Aza treatment (Fig. 5F–H and Fig. 6A–D, $p < 0.05$). Further investigation revealed that MTHFD2 knockdown aggravated the LPS-induced reduction in cell viability and MMP, and increase in apoptosis and ROS (Fig. 5F–H and Fig. 6A–D, $p < 0.05$). However, CTCF overexpression mitigated the effects of MTHFD2 knockdown on apoptosis, MMP, and ROS levels ($p < 0.001$), although it did not significantly restore cell viability (Fig. 5F–H and Fig. 6A–D). Therefore, MTHFD2 regulates CTCF promoter methylation and forms a pathogenic feedback loop in LPS-stimulated HK-2 cells.

Discussion

In this study, we found that the silencing of CTCF significantly exacerbated the reduction in cell viability and the increase in apoptosis in an LPS-induced AKI cell model. Notably, CTCF knockdown also intensified ROS accumulation and the loss of MMP, two classical indicators of mitochondrial function. This is the first study to demonstrate that CTCF exerts a protective role in maintaining mitochondrial homeostasis during sepsis-induced AKI. Previous studies have shown that excessive ROS generation can directly disrupt mitochondrial membrane integrity, triggering programmed cell death [26], while MMP loss is a key early event in mitochondrial damage and apoptosis [27]. Elevated ROS resulting from mitochondrial injury also contributes to tubular epithelial cell apoptosis [28]. Moreover, imbalance in ROS and MMP homeostasis has been recognized as a crucial mechanism underlying sepsis-induced kidney injury [29]. Collectively, our results suggested that CTCF may exert a protective effect on mitochondrial function by stabilizing ROS levels and MMP.

Further investigation revealed that overexpression of EP300 could partially reverse the CTCF silencing-triggered mitochondrial dysfunction, restoring MMP levels and reducing ROS accumulation. EP300 is a well-characterized histone acetyltransferase (HAT) that plays a pivotal role in epigenetic regulation during various physiological and pathological processes [30]. It catalyzes acetylation at lysine 27 of histone H3 (H3K27), forming H3K27ac, an epigenetic marker associated with active gene transcription [31]. Mechanistically, CTCF was found to bind strongly to EP300, indicating that CTCF may regulate mitochondrial function by recruiting EP300 and activating downstream gene transcription. Previous research has reported that EP300-mediated H3 acetylation promotes the expression of MTHFD2, thereby alleviating mitochondrial dysfunction in LPS-treated renal tubular epithelial cells [7]. Consistently, our data showed strong enrichment of H3K27ac and EP300 at the promoter region of MTHFD2 in HK-2 cells, supporting a robust epigenetic mechanism by which EP300 enhances MTHFD2 transcription.

DNA methylation represents another critical epigenetic regulatory mechanism involved in controlling gene expression. In our sepsis-induced AKI model, we observed a significant increase in DNA methylation levels at the CTCF promoter. Knockdown of MTHFD2 exacerbated the LPS-induced hypermethylation at the CTCF promoter, suggesting that MTHFD2 may maintain CTCF expression by modulating DNA methylation. Functional experiments further demonstrated that silencing MTHFD2 worsened mitochondrial dysfunction phenotypes, including MMP loss and ROS accumulation, whereas CTCF overexpression partially reversed these effects. These findings establish CTCF as a critical node within a feedback loop, where its expression is modulated by feedback from its downstream target, MTHFD2, via promoter methylation. Importantly, MTHFD2 is a vital enzyme in folate metabolism, and disruption of folate metabolism is implicated in the pathogenesis of kidney diseases [13,32]. Moreover, folate serves as an essential micronutrient for DNA

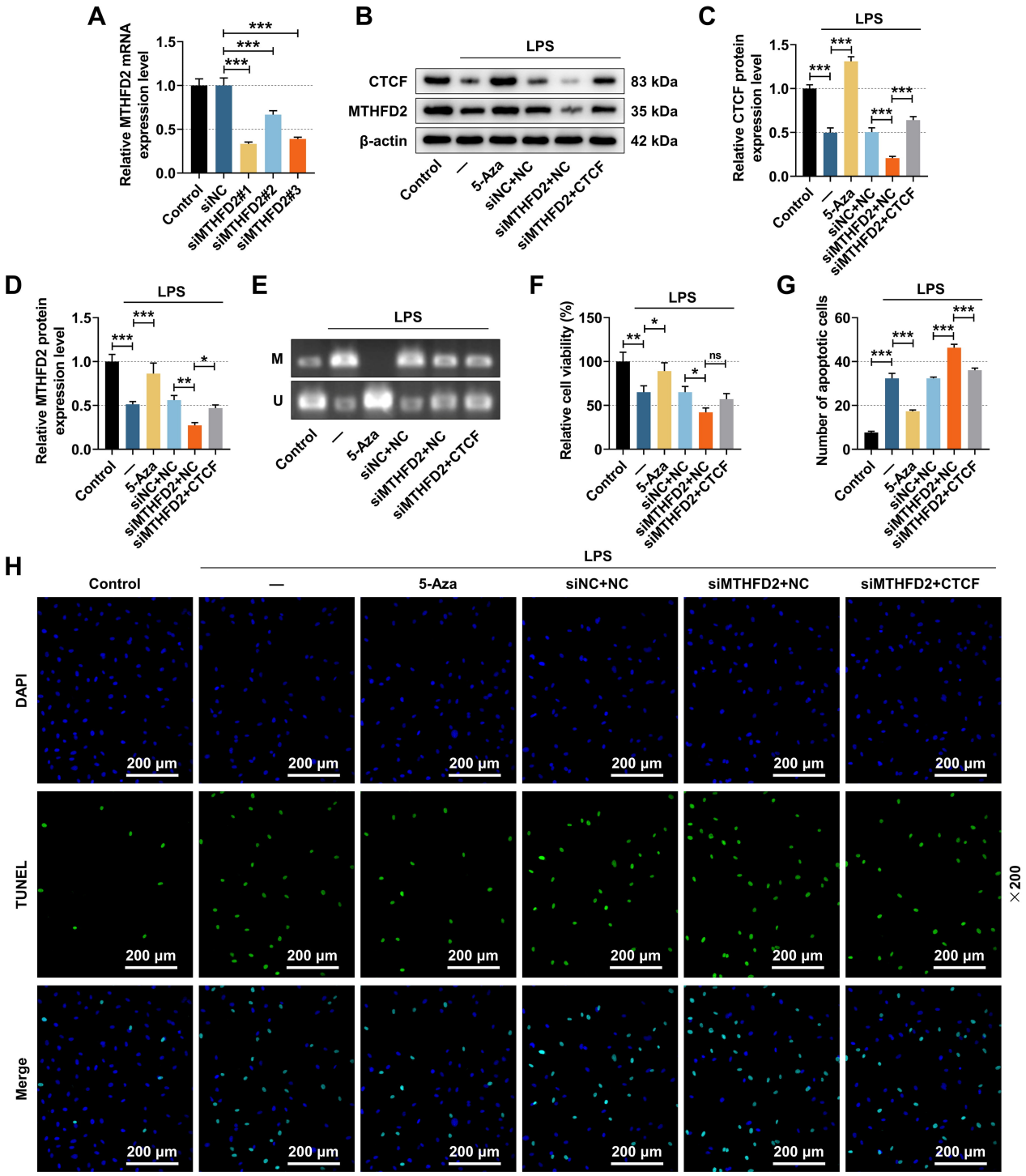

Fig. 5. MTHFD2 regulated CTCF methylation and influenced viability, and apoptosis in LPS-treated HK-2 cells. (A) qRT-PCR analysis on the efficiency of siRNA (siMTHFD2) knocking down *MTHFD2* in HK-2 cells. *β-actin* was used as the internal control. (B–D) Western blot analysis of CTCF and MTHFD2 protein levels in HK-2 cells from the Control, LPS, LPS+5-Aza-2′-deoxycytidine (5-Aza), LPS+siNC+NC, LPS+siMTHFD2+NC, and LPS+siMTHFD2+CTCF groups. β-actin served as the loading control. (E) Methylation-specific PCR analysis of CTCF methylation levels in HK-2 cells from the Control, LPS, LPS+5-Aza, LPS+siNC+NC, LPS+siMTHFD2+NC, and LPS+siMTHFD2+CTCF groups. (F) MTT assay to measure HK-2 cell viability in the Control, LPS, LPS+5-Aza, LPS+siNC+NC, LPS+siMTHFD2+NC, and LPS+siMTHFD2+CTCF groups. (G,H) TUNEL assay to test apoptosis in the Control, LPS, LPS+5-Aza, LPS+siNC+NC, LPS+siMTHFD2+NC, and LPS+siMTHFD2+CTCF groups. Green indicates TUNEL-positive cells; magnification: 200×; scale bar = 200 μm. All experiments were independently repeated three times. $^{*}p < 0.05$, $^{**}p < 0.01$, $^{***}p < 0.001$. ns, no significance.

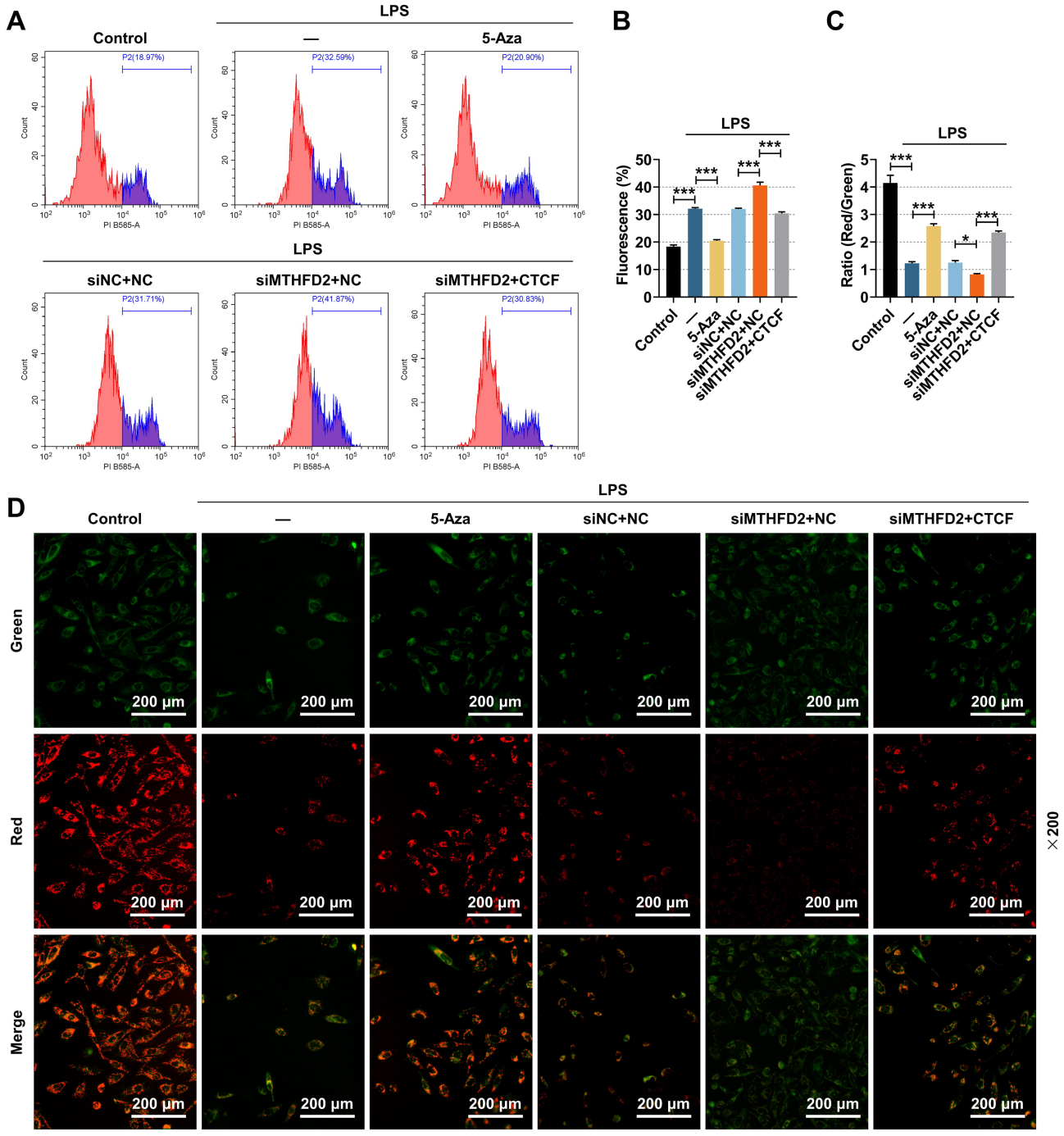

Fig. 6. CTCF and MTHFD2 impacted ROS production and mitochondrial membrane potential in LPS-induced HK-2 cells. (A,B) Flow cytometry analysis of ROS levels in the Control, LPS, LPS+5-Aza, LPS+siNC+NC, LPS+siMTHFD2+NC, and LPS+siMTHFD2+CTCF groups. (C,D) JC-1 staining to detect mitochondrial membrane potential across the Control, LPS, LPS+5-Aza, LPS+siNC+NC, LPS+siMTHFD2+NC, and LPS+siMTHFD2+CTCF groups. Magnification: 200×; scale bar = 200 μm. All experiments were independently repeated three times. $^{*}p < 0.05$, $^{***}p < 0.001$.

methylation reactions by providing methyl donors such as S-adenosylmethionine (SAM) [33]. Therefore, dysregulated folate metabolism may modulate CTCF promoter methylation and thereby influence its transcriptional expression and its capacity to recruit EP300. This could result in downregulation of MTHFD2, forming a self-reinforcing negative feedback loop. Taken together, our findings delineate a coherent but self-amplifying pathway in septic injury: The initial insult (LPS) triggers CTCF promoter hypermethylation, suppressing its expression and thereby its ability to activate MTHFD2 via EP300. The resulting decrease in MTHFD2 may then, through metabolic-epigenetic

crosstalk, further promote CTCF hypermethylation, forming a self-reinforcing vicious cycle that perpetuates mitochondrial dysfunction. This vicious cycle links metabolic enzyme dysfunction with epigenetic dysregulation and ultimately exacerbates mitochondrial damage. These findings reveal a novel epigenetic-metabolic feedback network underlying sepsis-induced AKI and identify the CTCF–EP300/MTHFD2 axis as a promising therapeutic target for restoring mitochondrial homeostasis.

This study has several limitations. First, all experiments were conducted in HK-2 cells, a human renal proximal tubular epithelial cell line. *In vivo* studies using appropriate animal models are needed to validate these findings and assess their physiological relevance. Second, although MTHFD2 is a key enzyme in folate metabolism, we did not directly analyze changes in folate metabolic intermediates or their contributions to epigenetic regulation in this model. Further exploration of folate dynamics and their functional roles in mitochondrial and epigenetic regulation will help deepen the understanding of this feedback mechanism.

Conclusion

In summary, our *in vitro* investigation using an LPS-stimulated human tubular cell model has uncovered a potential epigenetic regulatory loop involving CTCF and the EP300/MTHFD2 axis. We demonstrate that CTCF silencing impairs MTHFD2 expression via reduced EP300-mediated histone acetylation, while MTHFD2 modulates CTCF promoter methylation. Collectively, these findings provide preliminary insights into the complex epigenetic regulation of mitochondrial homeostasis in tubular cells and suggest that targeting the CTCF-EP300-MTHFD2 axis might hold therapeutic potential for mitigating sepsis-induced renal injury. Further validation in more complex models is warranted to confirm its pathophysiological relevance.

Availability of Data and Materials

The datasets used and/or analyzed during the current study are available from the corresponding author upon reasonable request.

Author Contributions

WH designed the research study, performed the experiments, collected and analyzed the data, drafted and revised the manuscript. WH reviewed and approved the final manuscript. WH agreed to accountable for all aspects of the work in ensuring that questions related to the accuracy or integrity of any part of the work are appropriately investigated and resolved.

Ethics Approval and Consent to Participate

Not applicable.

Acknowledgment

Not applicable.

Funding

This work was supported by the Zhejiang Province Medical and Health Science and Technology Program [grant number: 2024KY1489].

Conflict of Interest

The author declares no conflict of interest.

References

[1] Cao M, Wang G, Xie J. Immune dysregulation in sepsis: experiences, lessons and perspectives. Cell Death Discovery. 2023; 9: 465. https://doi.org/10.1038/s41420-023-01766-7.

[2] Kumar NR, Balraj TA, Kempegowda SN, Prashant A. Multidrug-Resistant Sepsis: A Critical Healthcare Challenge. Antibiotics (Basel, Switzerland). 2024; 13: 46. https://doi.org/10.3390/antibiotics13010046.

[3] Zarbock A, Nadim MK, Pickkers P, Gomez H, Bell S, Joannidis M, *et al*. Sepsis-associated acute kidney injury: consensus report of the 28th Acute Disease Quality Initiative workgroup. Nature Reviews. Nephrology. 2023; 19: 401–417. https://doi.org/10.1038/s41581-023-00683-3.

[4] Zhao L, Hao Y, Tang S, Han X, Li R, Zhou X. Energy metabolic reprogramming regulates programmed cell death of renal tubular epithelial cells and might serve as a new therapeutic target for acute kidney injury. Frontiers in Cell and Developmental Biology. 2023; 11: 1276217. https://doi.org/10.3389/fcell.2023.1276217.

[5] Zhu Z, Hu J, Chen Z, Feng J, Yang X, Liang W, *et al*. Transition of acute kidney injury to chronic kidney disease: role of metabolic reprogramming. Metabolism: Clinical and Experimental. 2022; 131: 155194. https://doi.org/10.1016/j.metabol.2022.155194.

[6] Zhao M, Wang Y, Li L, Liu S, Wang C, Yuan Y, *et al*. Mitochondrial ROS promote mitochondrial dysfunction and inflammation in ischemic acute kidney injury by disrupting TFAM-mediated mtDNA maintenance. Theranostics. 2021; 11: 1845–1863. https://doi.org/10.7150/thno.50905.

[7] Hu D, Sheeja Prabhakaran H, Zhang YY, Luo G, He W, Liou YC. Mitochondrial dysfunction in sepsis: mechanisms and therapeutic perspectives. Critical Care (London, England). 2024; 28: 292. https://doi.org/10.1186/s13054-024-05069-w.

[8] Wang Y, Zhu J, Liu Z, Shu S, Fu Y, Liu Y, *et al*. The PINK1/PARK2/optineurin pathway of mitophagy is activated for protection in septic acute kidney injury. Redox Biology. 2021; 38: 101767. https://doi.org/10.1016/j.redox.2020.101767.

[9] Ye W, Miao Q, Xu G, Jin K, Li X, Wu W, *et al*. CircRNA itchy E3 ubiquitin protein ligase improves mitochondrial dysfunction in sepsis-induced acute kidney injury by targeting microRNA-214-3p/ATP-binding cassette A1 axis. Renal Failure. 2023; 45: 2261552. https://doi.org/10.1080/0886022X.2023.2261552.

[10] Nilsson R, Jain M, Madhusudhan N, Sheppard NG, Strittmatter

L, Kampf C, *et al*. Metabolic enzyme expression highlights a key role for MTHFD2 and the mitochondrial folate pathway in cancer. Nature Communications. 2014; 5: 3128. https://doi.org/10.1038/ncomms4128.

[11] Yue L, Pei Y, Zhong L, Yang H, Wang Y, Zhang W, *et al*. Mthfd2 Modulates Mitochondrial Function and DNA Repair to Maintain the Pluripotency of Mouse Stem Cells. Stem Cell Reports. 2020; 15: 529–545. https://doi.org/10.1016/j.stemcr.2020.06.018.

[12] Zhu Z, Kiang KMY, Li N, Liu J, Zhang P, Jin L, *et al*. Folate enzyme MTHFD2 links one-carbon metabolism to unfolded protein response in glioblastoma. Cancer Letters. 2022; 549: 215903. https://doi.org/10.1016/j.canlet.2022.215903.

[13] Xu T, Zhang K, Shi J, Huang B, Wang X, Qian K, *et al*. MicroRNA-940 inhibits glioma progression by blocking mitochondrial folate metabolism through targeting of MTHFD2. American Journal of Cancer Research. 2019; 9: 250–269.

[14] Sun T, Cao Y, Huang T, Sang Y, Dai Y, Tao Z. Comprehensive analysis of fifteen hub genes to identify a promising diagnostic model, regulated networks, and immune cell infiltration in acute kidney injury. Journal of Clinical Laboratory Analysis. 2022; 36: e24709. https://doi.org/10.1002/jcla.24709.

[15] Durbin AD, Wang T, Wimalasena VK, Zimmerman MW, Li D, Dharia NV, *et al*. EP300 Selectively Controls the Enhancer Landscape of MYCN-Amplified Neuroblastoma. Cancer Discovery. 2022; 12: 730–751. https://doi.org/10.1158/2159-8290.CD-21-0385.

[16] Lazniewski M, Dawson WK, Rusek AM, Plewczynski D. One protein to rule them all: The role of CCCTC-binding factor in shaping human genome in health and disease. Seminars in Cell & Developmental Biology. 2019; 90: 114–127. https://doi.org/10.1016/j.semcdb.2018.08.003.

[17] Liu Y, Wang X, Zhu Y, Cao Y, Wang L, Li F, *et al*. The CTCF/LncRNA-PACERR complex recruits E1A binding protein p300 to induce pro-tumour macrophages in pancreatic ductal adenocarcinoma via directly regulating PTGS2 expression. Clinical and Translational Medicine. 2022; 12: e654. https://doi.org/10.1002/ctm2.654.

[18] Siegler BH, Altvater M, Thon JN, Neuhaus C, Arens C, Uhle F, *et al*. Postoperative abdominal sepsis induces selective and persistent changes in CTCF binding within the MHC-II region of human monocytes. PloS One. 2021; 16: e0250818. https://doi.org/10.1371/journal.pone.0250818.

[19] Shih CC, Hii HP, Tsao CM, Chen SJ, Ka SM, Liao MH, *et al*. Therapeutic Effects of Procainamide on Endotoxin-Induced Rhabdomyolysis in Rats. PloS One. 2016; 11: e0150319. https://doi.org/10.1371/journal.pone.0150319.

[20] Fila M, Chojnacki C, Chojnacki J, Blasiak J. Is an "Epigenetic Diet" for Migraines Justified? The Case of Folate and DNA Methylation. Nutrients. 2019; 11: 2763. https://doi.org/10.3390/nu11112763.

[21] Sun M, Li J, Mao L, Wu J, Deng Z, He M, *et al*. p53 Deacetylation Alleviates Sepsis-Induced Acute Kidney Injury by Promoting Autophagy. Frontiers in Immunology. 2021; 12: 685523. https://doi.org/10.3389/fimmu.2021.685523.

[22] Xiao X, Tang W, Yuan Q, Peng L, Yu P. Epigenetic repression of Krüppel-like factor 4 through Dnmt1 contributes to EMT in renal fibrosis. International Journal of Molecular Medicine. 2015; 35: 1596–1602. https://doi.org/10.3892/ijmm.2015.2189.

[23] Kagan AB, Garrison DA, Anders NM, Webster JA, Baker SD, Yegnasubramanian S, *et al*. DNA methyltransferase inhibitor exposure-response: Challenges and opportunities. Clinical and Translational Science. 2023; 16: 1309–1322. https://doi.org/10.1111/cts.13548.

[24] Huang L, Li L, Cheng B, Xing T. SLC38A6, regulated by EP300-mediated modifications of H3K27ac, promotes cell proliferation, glutamine metabolism and mitochondrial respiration in hepatocellular carcinoma. Carcinogenesis. 2022; 43: 885–894. https://doi.org/10.1093/carcin/bgac061.

[25] Zhu Q, Wang J, Zhang W, Zhu W, Wu Z, Chen Y, *et al*. Whole-Genome/Exome Sequencing Uncovers Mutations and Copy Number Variations in Primary Diffuse Large B-Cell Lymphoma of the Central Nervous System. Frontiers in Genetics. 2022; 13: 878618. https://doi.org/10.3389/fgene.2022.878618.

[26] Zheng D, Liu J, Piao H, Zhu Z, Wei R, Liu K. ROS-triggered endothelial cell death mechanisms: Focus on pyroptosis, parthanatos, and ferroptosis. Frontiers in Immunology. 2022; 13: 1039241. https://doi.org/10.3389/fimmu.2022.1039241.

[27] Park C, Cha HJ, Kim MY, Bang E, Moon SK, Yun SJ, *et al*. Phloroglucinol Attenuates DNA Damage and Apoptosis Induced by Oxidative Stress in Human Retinal Pigment Epithelium ARPE-19 Cells by Blocking the Production of Mitochondrial ROS. Antioxidants (Basel, Switzerland). 2022; 11: 2353. https://doi.org/10.3390/antiox11122353.

[28] Su L, Zhang J, Gomez H, Kellum JA, Peng Z. Mitochondria ROS and mitophagy in acute kidney injury. Autophagy. 2023; 19: 401–414. https://doi.org/10.1080/15548627.2022.2084862.

[29] Wu M, Huang Z, Akuetteh PDP, Huang Y, Pan J. Eriocitrin prevents Sepsis-induced acute kidney injury through anti-inflammation and anti-oxidation via modulating Nrf2/DRP1/OPA1 signaling pathway. Biochimica et Biophysica Acta. General Subjects. 2024; 1868: 130628. https://doi.org/10.1016/j.bbagen.2024.130628.

[30] Kanada R, Kagoshima Y, Asano M, Suzuki T, Murata T, Haruta M, *et al*. Discovery of EP300/CBP histone acetyltransferase inhibitors through scaffold hopping of 1,4-oxazepane ring. Bioorganic & Medicinal Chemistry Letters. 2022; 66: 128726. https://doi.org/10.1016/j.bmcl.2022.128726.

[31] Sankar A, Mohammad F, Sundaramurthy AK, Wang H, Lerdrup M, Tatar T, *et al*. Histone editing elucidates the functional roles of H3K27 methylation and acetylation in mammals. Nature Genetics. 2022; 54: 754–760. https://doi.org/10.1038/s41588-022-01091-2.

[32] Doi K, Leelahavanichkul A, Hu X, Sidransky KL, Zhou H, Qin Y, *et al*. Pre-existing renal disease promotes sepsis-induced acute kidney injury and worsens outcome. Kidney International. 2008; 74: 1017–1025. https://doi.org/10.1038/ki.2008.346.

[33] Socha MW, Flis W, Wartęga M. Epigenetic Genome Modifications during Pregnancy: The Impact of Essential Nutritional Supplements on DNA Methylation. Nutrients. 2024; 16: 678. https://doi.org/10.3390/nu16050678.